



The Challenge of Predicting OAG Progression from the Initial Visual Field Test

Aristeidis Chandrinos^{1*}

¹Department of Biomedical Sciences, Division of Optics and Optometry, Laboratory of Optical Metrology, School of Health and Welfare, University of West Attica, Egaleo Park Campus, Athens, Greece.

Author's contribution

The sole author designed, analysed, interpreted and prepared the manuscript.

Article Information

Editor(s):

(1) Dr. Panagiotis Tsikripis, University of Athens, Greece.

Reviewers:

(1) Mahesh B. Mawale, Kavikulguru Institute of Technology and Science, India.

(2) Seema Dutt Bandhu, Punjab Institute of Medical Sciences, India.

Complete Peer review History: <http://www.sdiarticle4.com/review-history/63816>

Original Research Article

Received 15 October 2020

Accepted 19 December 2020

Published 16 January 2021

ABSTRACT

Purpose: The aim of this study was the development of a critical code in order to combine statistics with a workable diagnostic system for open angle glaucoma that could predict improvement or deterioration of the tested visual field of a glaucoma suspect, most likely after the first or second visit for the visual field test.

Methods: The study plan was to apply a set of different filters in order to select the most efficient one that could remove the most of the noise of the test printout, of which probably the greater part of this removed noise could be the component of the learning effect, as it was expected to be at the first or second session. The common mean and median filters were initially used and later on an adapted or Hybrid filter was designed in MatLab© environment and in a similar philosophy to Gardiner's Predictor filter. Taking into account the details of the study data, an Adaptive or Hybrid filter following the deployment of the optic nerve fibre layers of the retina was tested and selecting different weight depending on the locations of possible glaucoma defects.

Results: Initially, the used mean and median filters, used to remove noise of visual field provided ambitious results. The first filter blurred the edges and the overall appearance looked fuzzy or blurry. The second one calculated the values of the neighbourhood and set these in ascending array. Then selected the median of these values to replace the original one. The result in general looks misleading. Next, applying the Hybrid Adapted filter, the end results illustrated elimination of

*Corresponding author: E-mail: achand@uniwa.gr;

measured noise in the visual field tests and likely the first visit outcome could predict the third or the fifth visit one.

Conclusion: This is a promising approach to identify and eliminate measurement noise in the visual field tests and to predict, after filtering the first examination outcome, the likely visual field outcome of the third or the fifth visit. The challenge of predicting the progression of open angle glaucoma from the initial visit nowadays is even more than any other the “Holy Grail” of Perimetry.

Keywords: Filters; open angle glaucoma; visual field signal; noise.

1. INTRODUCTION

1.1 Signal and Noise Relationship

A signal can be defined as the physical carrier of information [1]. By and large, a signal is an official description of an observable fact that evolves time or space [2]. By signal processing any manual or “mechanical” operation could be designated, which may modify, analyse or otherwise manipulate the information contained in a signal [3].

A signal mathematically can be represented in various ways. A natural representation of a signal is a function $f(x)$, where x denotes a variable. The representation of light waves carrying information from a scene to the eye is quite complicated but the final image is simply represented as a function of two variables $f(x,y)$. For example, in a black and white image the (x,y) is the spatial location of the point in the image and $f(x,y)$ is the brightness value of that point. A colour image is represented as a vector valued function $[R(x,y), G(x,y) \text{ and } B(x,y)]$, where R , G and B are the intensities of red, green and blue colours, respectively [1,4].

A rough division of signal problems may include three phases. The first is the removal of interference, the second may be the signal transformation to another form and finally the analysis and extraction of some characteristics [5].

Noise in the majority of signal systems is a product of both internal and external sources to the system. All measurements in the real world are bothered by noise. In fact, a noisy signal consists of electronic noise, but can also incorporate external procedures that affect the considered phenomenon — wind, vibrations, differences of temperature, deviation of humidity, etc., and depend on the measured matter and on the sensitivity of the device of measurement [4-6].

Signal-to-noise ratio is a determination used in science to compute how much a signal has been

distorted by noise. It is the relation between signal strength and the noise influence, which distorts the signal. It is recognized as the power ratio between the significant information (signal) and the useless signal (noise): In practice, if the transmitted signal falls below the level of the noise in the system, data can no longer be decoded or evaluated by the receiver [7]. More often than not, it is possible to decrease the noise if you control the environment or the source event. Mainly this could be done using different types of filters [4,8].

The objective of any type of filter is to extract the noise that has distorted the signal. Generally it is based on a statistical approach. However, the design of some filters takes a different approach. One filter design makes it possible to have data of the properties of both the initial signal and the noise, and another one may look for the output that would come as close to the unique signal as possible [9].

1.2 Common Types of Filters

Mean filtering is a simple, spontaneous and easy to implement method of smoothing results, i.e. reducing the amount of intensity variation between one value and the next. Often it is based around a 3×3 square kernel (Fig.1), which represents the shape and size of the neighbourhood to be sampled when calculating the mean. The Mean filter replaces each pixel value in a system with the mean or the average value of its neighbours, including itself. This has the effect of eliminating values that are unrepresentative of their surroundings [10].

Two main problems are evident with mean filtering. Firstly that a single location with a very misleading value, can significantly affect the mean value of all the other locations in its neighbourhood, and secondly, when the filter neighbourhood overlaps an edge, the filter will interpolate new values for locations on the edge, as we require sharp edges in the output and so the filter will blur that edge and the overall appearance may look fuzzy or blurry [10,11].

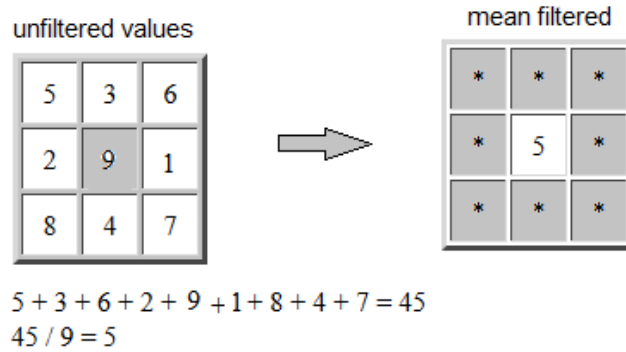


Fig. 1. Schematic representation of mean filtering in a 3X3 kernel, where after the summation of the values of the neighbourhood, they are divided by the total number of pixels and the result value replaces the original one

One more common non-linear filtering technique, used to remove noise, employs the median filter. Median filtering is extensively applied in digital processing as it maintains edges while getting rid of noise. This technique calculates the median of the surrounding locations to determine the new value of the location. A window of size 3*3 is taken (Fig. 2). The nine elements in this window are stored in an array and then these elements are sorted in ascending order of their pixel values. The median is calculated from these sorted pixels and then the centre element of the 3*3 kernel is replaced by this median value [11].

Weighted Median (WM) filters are another type of filters, which have the robustness and edge preserving capability of the classical median filter and are similar to linear filters in certain properties. In WM filtering a window of a 3X3 kernel is used (Fig. 3) in the example shown. All nine value of the neighbourhood are multiplied by the nine corresponding values of the weight. The summation of these nine products divided by the total weight gives the filtered value to replace the respective initial pixel value. Weighted Median filters belong to the broad class of non-linear filters and enable noise attenuation capability, where intensity values are examined and depending on the range of intensity, particular weights are multiplied [12].

1.3 Aim of the Study

The design of this study involved performance evaluation of different filters on visual field output. The critical arrangement was to develop a code to combine statistics with a workable

diagnostic system that is capable of detecting deterioration of visual field in the early stages of glaucoma. Moreover, to develop a system that could predict improvement or deterioration of the tested visual field of a glaucoma suspect, most likely after the first or second visit and not to expect to conclude after the completion of the fifth visit assessment.

In other words, the plan was to apply a set of different filters in order to select the most efficient one that could remove the most of the noise of the test printout, of which probably the greater part of this removed noise could be the component of the learning effect, as it was expected to be at the first or second session. The common mean and median filters were initially used and later on an adapted or Hybrid filter was designed in a similar philosophy to Gardiner's Predictor filter. In case of real visual field deterioration, as in most of the OAG patients' printouts, the filter expected not to denoise much learning, as the defected locations could not learn any more.

1.4 Sample

The sample consisted of 79 consecutively presenting individuals, coming from author's previous research carried out in accordance to the tenets of the Declaration of Helsinki. Included 25 open angle glaucoma (OAG) patients, 25 ocular hypertensive (OHT) subjects and 29 normal individuals, as a control set [13]. All these data collected and transformed in computer files, in a mode that MatLab© could easily use all information coming from the 790 printouts of the whole cohort.

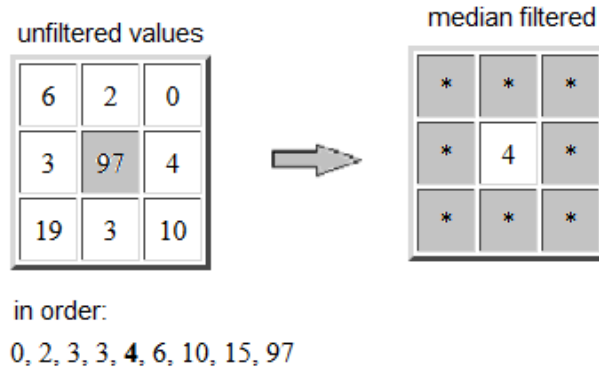


Fig. 2. Schematic representation of median filtering in a 3X3 kernel where after setting the values of the neighbourhood in ascending array the median of these values is selected to replace the original one

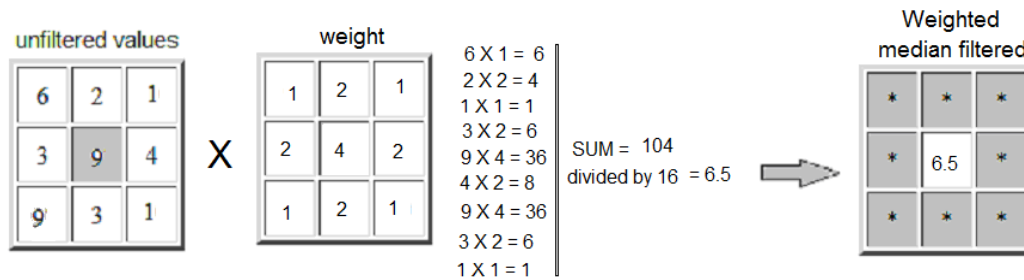


Fig. 3. Schematic representation of weighted median filtering in a 3X3 kernel, after multiplying the neighbourhood values with the corresponding weights the summation is divided by the overall weight and the resulting value replaces the original one

The design of the study included analysis of numerous single visual field printouts coming from a cohort of normal individuals that were naïve to any type of perimetry and could be expected to improve over the five sessions for all types of perimetry and of OAG patients that would improve over the five visits for the SITA algorithms, except SITA Standard given their previous experience [13].

The OHT individuals were excluded from the study, mainly because these individuals were quite experienced in SITA Standard and SITA Fast algorithms and were not expecting to learn any more for these algorithms [14].

2. METHODS

2.1 Filtering the Perimetric Results

Automated perimetry is widely used for the detection and follow up of glaucomatous field loss. The most important component of

perimetric estimation is the assessment of the pointwise sensitivity or threshold variation in visual field data [15,16]. Especially the early glaucomatous field loss is characterised by this variability and fluctuation [17,18].

The Humphrey Field Analyser (HFA) is typical of advanced automated perimeters in providing the clinician with a series of mechanisms to quantify and interpret this pointwise sensitivity variation and threshold fluctuation [16]. The Single Field Analysis printout illustrates a numeric sensitivity chart, on the left of the greyscale graph, for the central 30 degrees of the eye field (Fig. 4). A signal is a sequence of functions of integers (f: z = R). So, the data i.e: 21, 22, 21, 19, 21, 23, 21, 24, 21, 19, 21, 20, ...if it is a sequence of real values, could be a signal. In the visual field numeric printout there are many sequences of different values [19].

This numeric chart if deployed as a series of values, following the location map as in Fig. 4, it

could be a signal, which may well be processed with any common filter to remove the unnecessary noise as in the block diagram in Fig. 5.

In MatLab© environment it is not difficult to design a modulus, a programming process, which is able to retrieve the data of OAG, OHT or normal subjects from a set of various VF printouts for all visits (see Appendix, modulus one) and then to calculate the action of the specific filter (see Appendix, modulus two for a median filter and three for an Hybrid filter) and draw the result in an analog visual field representation following the corresponding table of sensitivity values of the visual field numeric chart to the data locations (Fig. 7), and then to redraw the comparison results between visits for the specific subject, the right eye and all the 5 visits (Figs 8 and 9).

This numeric chart if deployed as a series of values, following the location map as in Fig. 4, it could be a signal, which may well be processed with any common filter to remove the unnecessary noise as in the block diagram in Fig. 5.

2.2 Previous Studies of Visual Field Filtering

Initially, Fitze et al, (1995) introduced a method of improving the repeatability of visual field data by applying techniques used in image processing [19]. Crabb and colleagues (1995) demonstrated a new framework for evaluating pointwise sensitivity variation in computerised visual field. Furthermore, Crabb and associates (1997) show

how the predictive performance of a method for determining glaucomatous progression in a series of visual fields can be improved by first subjecting the data to a spatial filtering technique [20].

They also concluded that the spatial filter decreases the number of false-positives when detecting progression by reducing the level of noise present. In addition, the filter increased the likelihood of detecting true deteriorating locations of the visual field and reduced the probability of flagging not viable defects [21].

In this method, the raw sensitivity value is replaced by one derived from a linear combination of the sensitivities at the nine points in a 3X3 square centered on the point of interest. This is repeated for each point in the field in turn, each time looking at the points in a square surrounding the point of interest [22].

Strouthidis and colleagues (2007) concluded that application of the spatial filter resulted in similar specificity but with a higher rate of detected progression. This filter may therefore be useful in the monitoring of glaucomatous progression as it may reduce the dependence on confirmatory testing, although it has yet to be applied to longitudinal SITA data [23].

Gardiner and associates (2004) tested a physiologically accurate spatial filter to be applied to the data after patient examination, by impeding the quantity of noise present in the readings [15]. A Virtual Eye computer simulation was used to test the filter.

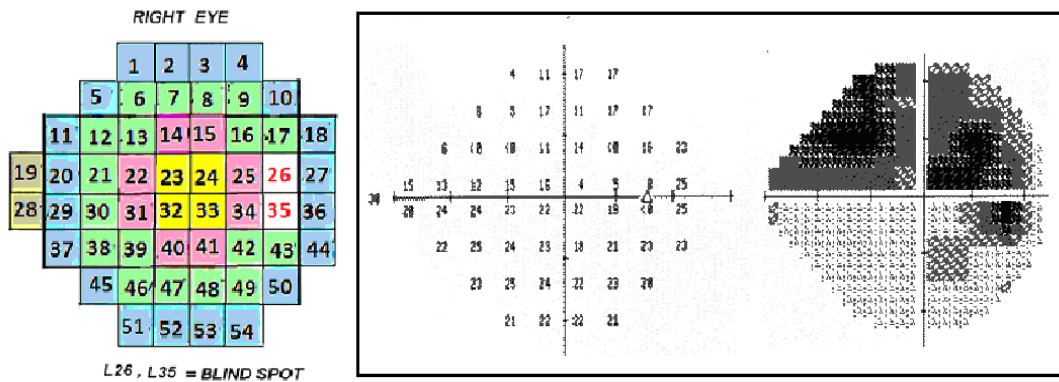


Fig. 4. The numeric chart of the HFA visual field output (middle) and the greyscale graph (right) and the corresponding table of sensitivity values of the visual field numeric chart to the data locations (left), for the right eye of a glaucoma patient (After Chandrinos A., 2017)

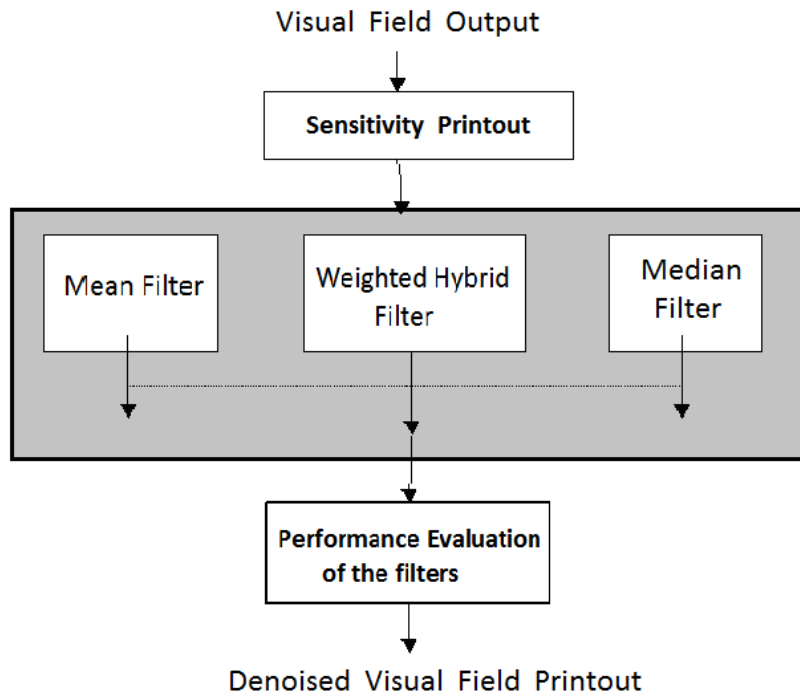


Fig. 5. Block diagram illustrates the phases of denoising visual field printout

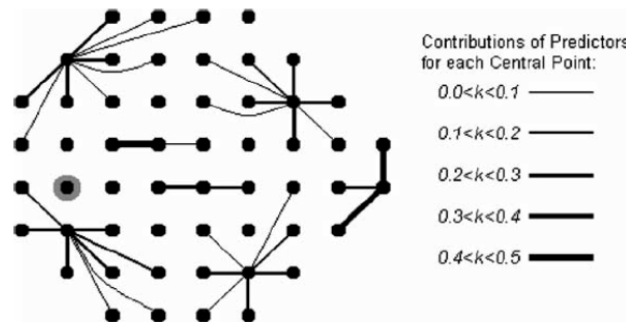


Fig. 6. Gardiner's proposed Predictor filter with the group of points connected with lines of different thickness, named as k-factor (right table) for the applied filter (after Gardiner et al., 2004)

The filter obeys the rules of the accepted physiological shape of the retinal nerve fibre layer. Fig.6 illustrates a few of the Central Points that are employed to the filter. If a point is connected to the Central Point by a line, it indicates that this point is a predictor for the Central Point [16]. As noted in the table at the right of the graph, the thicker the line, the larger the effect it has on the prediction. The remaining contribution to the filtered value comes from the

Central Point itself. It is seen that predictors are not necessarily neighbours of the Central Point (as they would be if the Gaussian filter was being considered), but they follow the expected arcs [16,22].

Additionally, the performance of Gardiner's filter, according to the study, was much better than the Gaussian filter. By the way, it was common for defects to be blurred out by the Gaussian filter.

To this point, this is really difficult given the inaccuracy of threshold perimetry (in terms of the high inter-test and intra-test variability) and the various components of variability (or noise) associated with the perimetric process [24,13].

3. RESULTS

Initially, two filters were designed and modified by integrating the well known mean and median filters in MatLab© (Version 7.5, 2007) environment that was used in previous similar studies, by coding the modules files for the appropriate applying method [20,14].

Afterwards, taking into account the details of the study data, an Adaptive or Hybrid filter was designed following the deployment of the optic nerve fibre layers of the retina (Fig. 7 at the right-top) and selecting different weight (Fig. 7, right column) depending on the locations of possible glaucoma defects, in proportion to the Garway-Heath and associates previous study [15,25].

3.1 Statistical Analysis

The sensitivity elevation discrepancy of raw data and data after the use of the adaptive filter for normal and OAG subjects are illustrated with box and whiskers plots in Fig. 10 and 11.

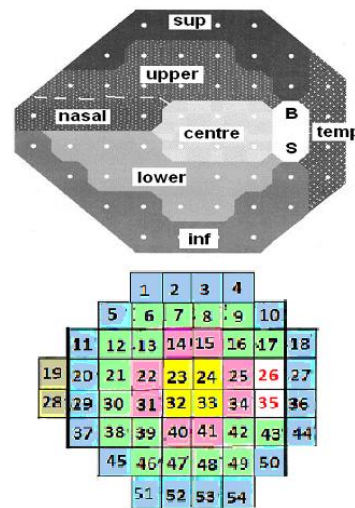
4. DISCUSSION

Commonly; it is believed that like in many psychophysical tests, the individual experience manipulates the results of automated perimetry [13].

In the present study results confirm that a visual field printout can be filtered to predict a close to the normal output of the field after three or five visits, if a special filter for the particular data could be designed. At the same time findings arise suggestions that learning effect or fatigue could probably mask these first visual field printouts and would likely improve in the next sessions [13].

In previous similar studies [15,20] researchers easily observed that the median filter preserves the edges much better than the mean filter. In the present study, the mean and median data were incorporated in MatLab environment in order to produce a new filter and the outcome demonstrated no blurring in the median filtered visual field output, while blurring was very visible in filtered visual field results by the mean filter, mainly in locations of visual field periphery [13]. Conversely, it was detected some edge shifts caused by the median filter. Subsequently, taking into account the deployment of the optic nerve fibre layers of the retina (Fig. 7), in a similar

Bundle Name	Group of Points	Weight
Superior bundle	sup=([1:5,9,10,17]);	(+/-3.01)
Upper bundle	upper=([6:8,11:16,]);	(+/-2.37)
Temporal bundle	temp=([18,27,36,44]);	(+/-1.60)
Central bundle	centre=([23:25,32:34]);	(+/-1.60)
Inferior bundle	inf=([37,43,45,46,49:54]);	(+/-2.27)
Lower bundle	lower=([28:31,38:42,47,48]);	(+/-2.37)
Nasal bundle	nasal=([19:22]);	(+/-2.37).....



Locations 26 and 35 = Blind Spot

Fig. 7. Graphic illustration of the design of a Hybrid filter according the deploying of the optic nerve bundles. The numbers of group points (middle column) all over the field follow the bundles of the retinal nerve fiber layers (after Garway-Heath et al., 2000) at the top-right of the illustration and the weight (right column) that was calculated from the sensitivity variation of the particular group of points in the retinal bundles

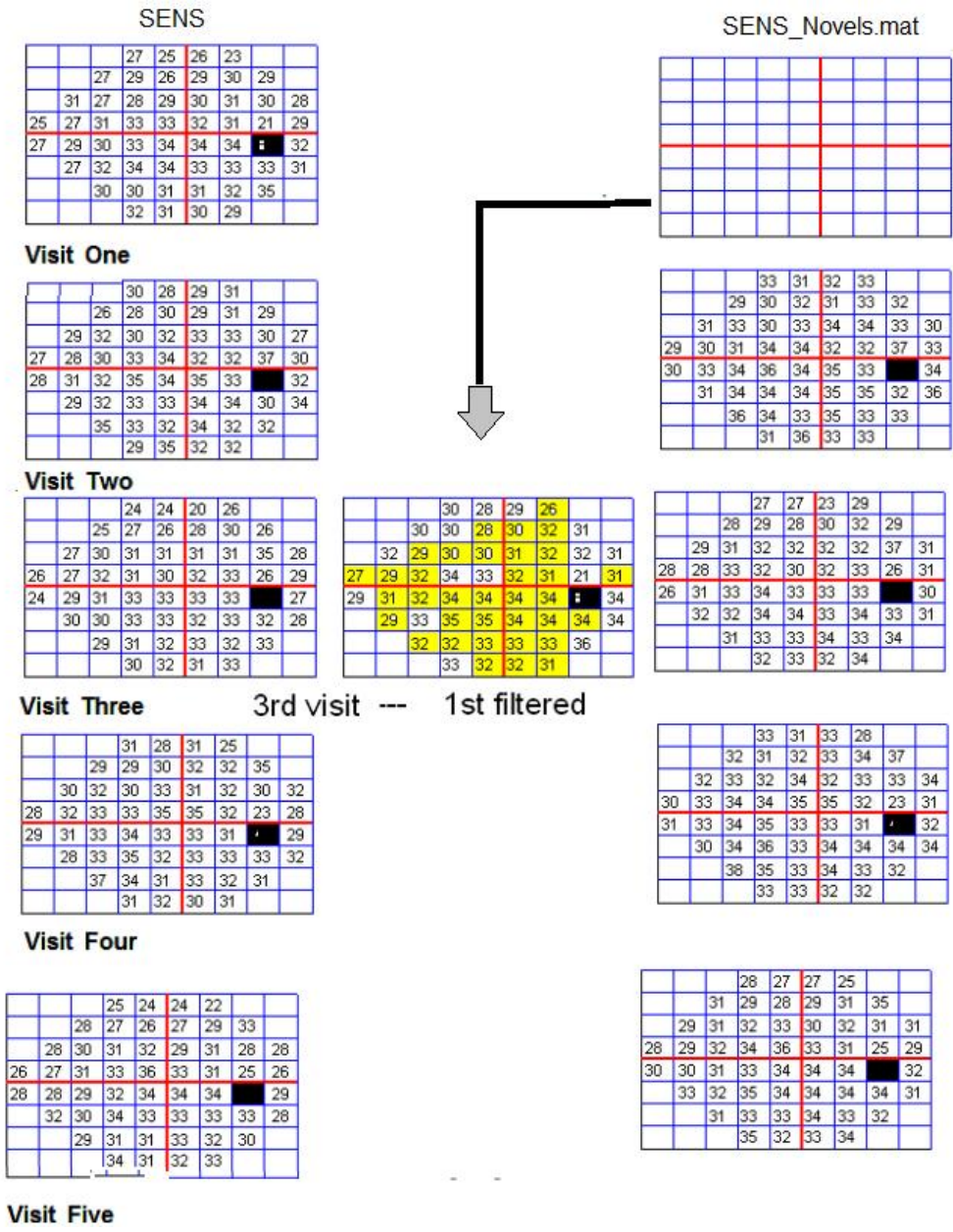


Fig. 8. Graphical representation of filtering results, for the right eye of a normal subject's visual field, for all visits and the SITA Standard algorithm. The left column illustrates the raw sensitivity values (SENS) and the right column the sensitivity values after applying the adaptive hybrid (SENSNovels.mat) filter. The 1st visit filtered outcome can be compared with the 3rd visit raw sensitivity chart, where the matching area of the visual field is coloured yellow (After Chandrinis A., 2017)

design of the Garway-Heath and associates study an Adaptive or Hybrid filter was designed again in MatLab and a promising issue of prediction of later test results (Figs. 8,9) was evident [14,25].

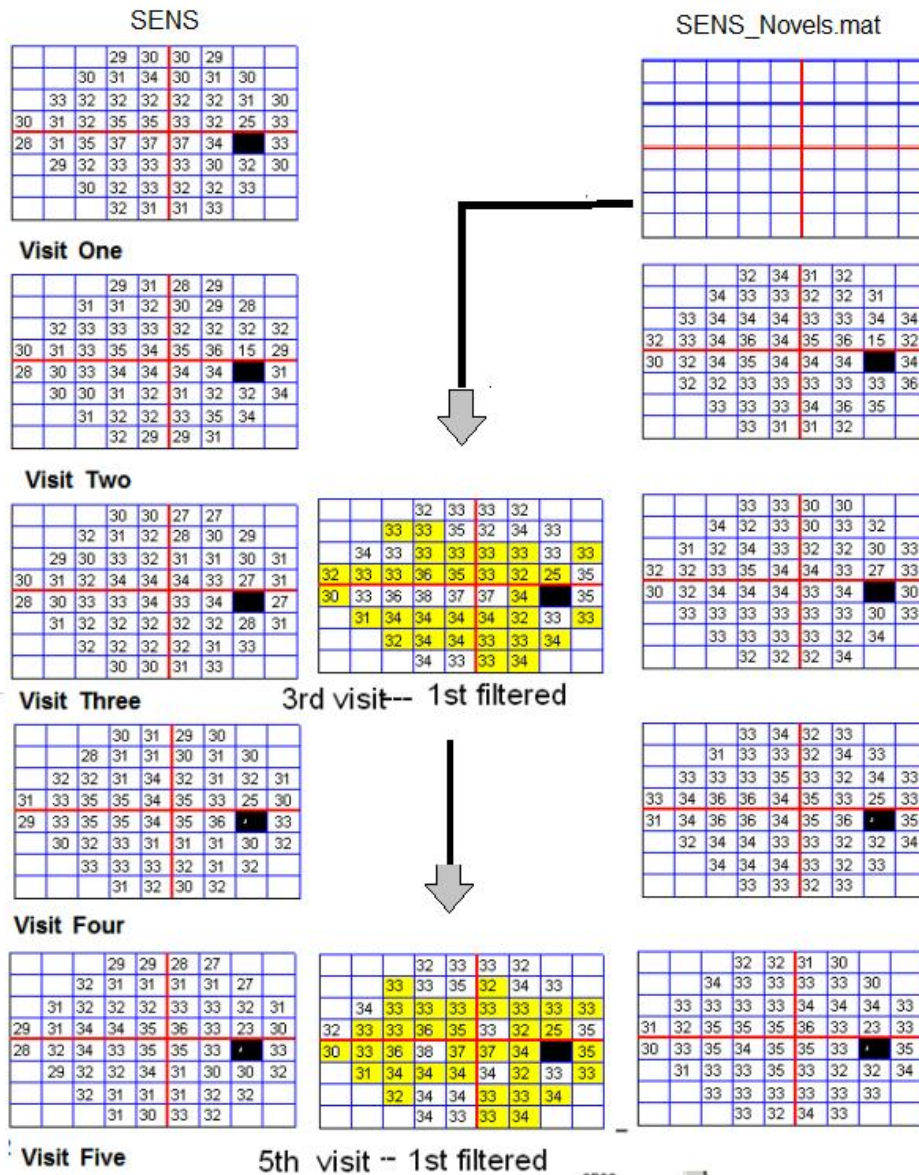


Fig. 9. Graphical representation of filtering results, for the right eye of a glaucoma patient's visual field (with mild defects), for all visits and the SITA Standard algorithm. The left column illustrates the raw sensitivity values (SENS) and the right column the sensitivity values after applying the adaptive hybrid (SENSNovels.mat) filter. The 1st visit filtered outcome can be compared with the 3rd visit raw and with the 5th visit raw sensitivity chart, where the matching areas of the visual field is coloured yellow (After Chandrinis A., 2017)

Evaluation between plots of sensitivity elevation discrepancy throughout the five visits (Figs.10,11), easy could reveal that the reduced learning effect may be a good indication of improvement in healthy individuals and in OAG patients [13,26]. Of course, it is important to emphasize that in these plots data comes only

from the right eye of the examined Individuals, given that healthy group were naïve of SAP and as a result they would experience minimum fatigue and glaucoma patients, as experienced in perimetry would have demonstrated also the least fatigue [26,27].

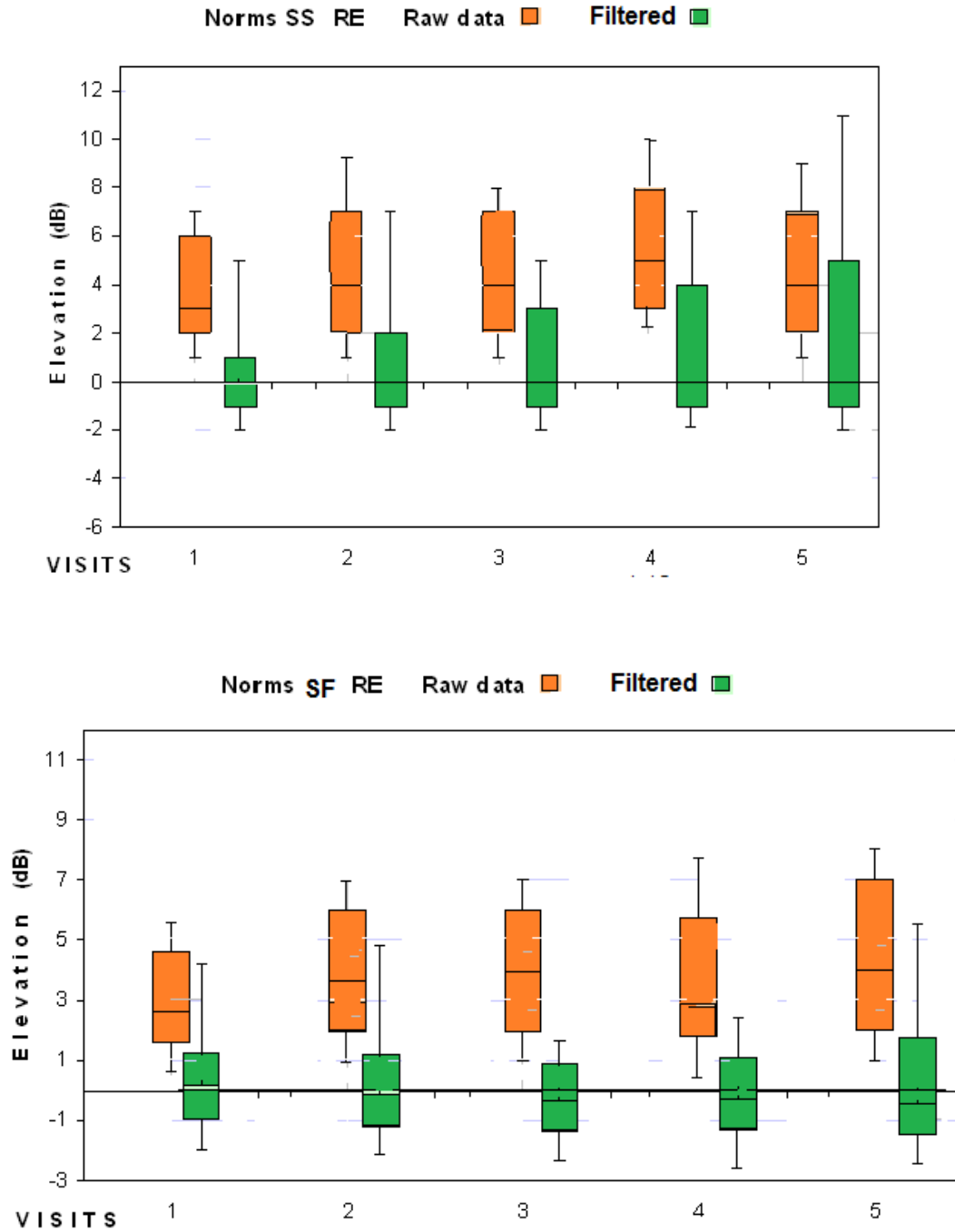


Fig. 10. Graphical illustration of the discrepancy of sensitivity elevation for the right eye of normal subjects of raw data (orange shade) and data after the use of the adaptive filter (green shade), for SITA Standard (Top) and SITA Fast (bottom) strategies, at all five visits (After Chandrinis A., 2017)

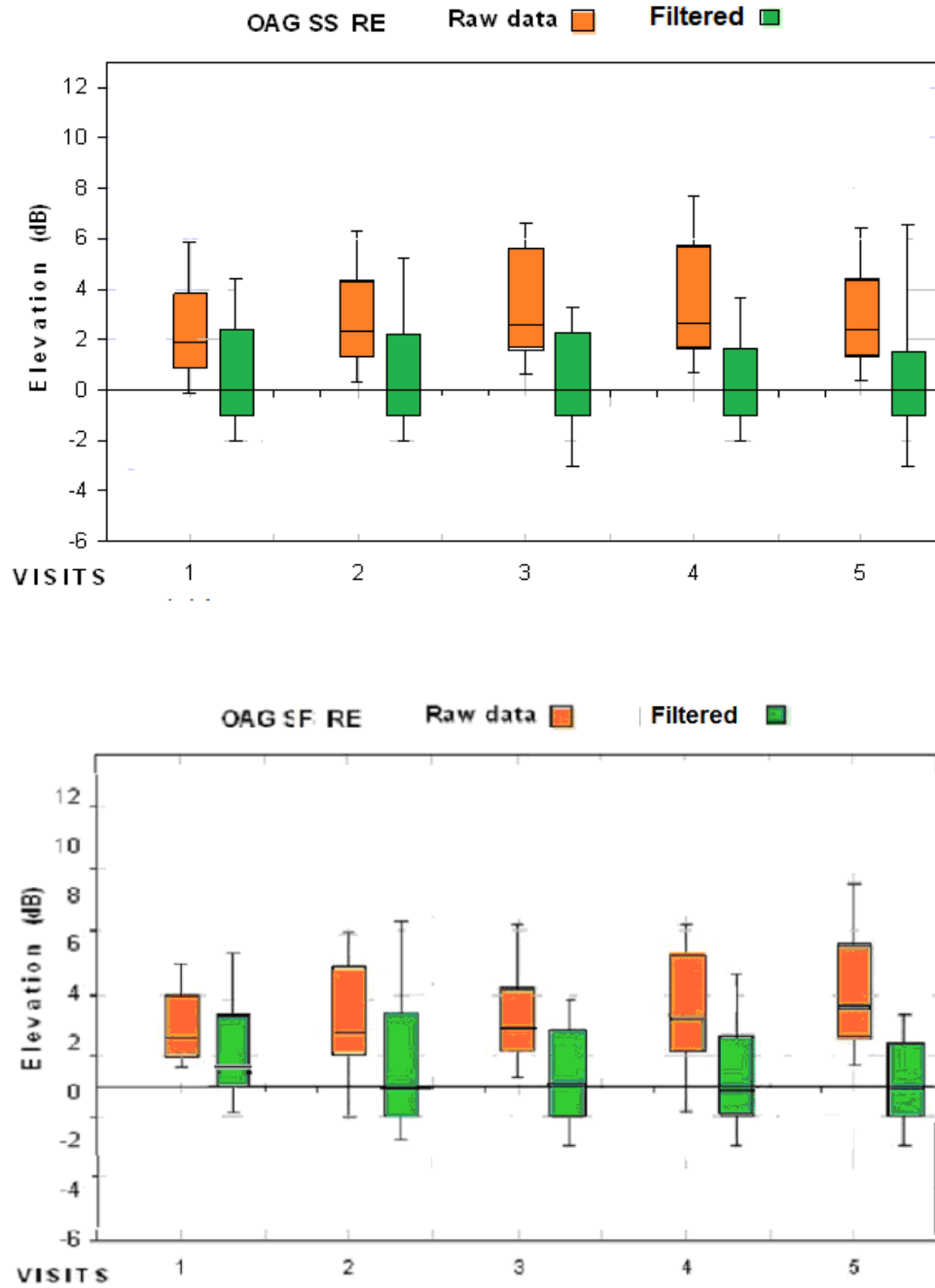


Fig. 11. Graphical illustration of the discrepancy of sensitivity elevation for the right eye of OAG patients of raw data (orange shade) and data after the use of the adaptive filter (green shade), for SITA Standard (Top) and SITA Fast (bottom) strategies, at all five visits (After Chandrinis A., 2017)

5. CONCLUSIONS

Probably, the most significant difficulty for the clinician is the tenacity of an unstable

psychophysical behaviour in variability (signal and noise) of the visual fields. The result from one test suggests that the patient is normal (no glaucoma), while the result from the other test

shows that the same patient may be abnormal (having glaucoma).

In present study, an alternative way of dealing with noisy data was introduced. A method of filtering the visual field results would be contemporary adaptive hybrid filters. This is a promising approach to identify and eliminate measurement noise in the visual field tests and to predict, after filtering the first examination outcome, (Figs.8,9) the likely visual field outcome of the third or the fifth visit.

The early indication of the glaucoma gives the clinician the opportunity for efficient treatment, comfort for the patient and minimal financial expenses for both the individual and the state or private insurance company. Although the past years a large amount of information has been obtained concerning the visual fields behaviour, the future gold standard of glaucoma test, is not yet available for the glaucoma patients at hand.

Even though predictive values could be more important in clinical practice, the parameters of accuracy are still more popular between perimetry-operators. The challenge of predicting the progression of open angle glaucoma from the initial visit, nowadays is even more than any other the "Holy Grail" of Perimetry.

CONSENT

It is not applicable.

ETHICAL APPROVAL

It is not applicable.

COMPETING INTERESTS

Author has declared that no competing interests exist.

REFERENCES

1. Astola J, Kuosmanen P. Fundamentals of nonlinear Digital Filtering. CRC Press; 1997.
2. Ruelle D. Diagnosis of dynamical systems with fluctuating parameters. Proc. R. Soc. London. 1987;A 413:5-8.
3. Baraniuk R. Signals and systems, the connexion project, Houston, USA; 2003.
4. Chandrinos A. Aspects of a perimetric learning index - Doctor of Philosophy Thesis, School of Optometry, Cardiff Un., Wales, UK; 2017.
5. Oppenheim A, Verghese G. Signals, systems and inference, MIT Class Notes, USA; 2010.
6. Barat V, Borodin Y, Kuzmin A. Intelligent AE signal filtering methods J. Acoustic Emission, , Moscow, 01000, Russia. 2010; 28:(129-131).
7. Gardiner SK, Fortune B, Demirel S. Signal-to-noise ratios for structural and functional tests in glaucoma. Transl Vis Sci Technol. 2013;2(6):3.
8. Jornitz MW. Filter construction and design. Adv Biochem Eng Biotechnol. 2006;98: 105-123.
9. Levy RV, Jornitz MW. Types of filtration. Adv Biochem Eng Biotechnol. 2006;98:1-26.
10. Senel HG, Peters RA 2nd, Dawant B. Topological median filters. IEEE Trans Image Process. 2002;11(2):89-104.
11. Green O. Efficient scalable median filtering using histogram-based operations. IEEE Trans Image Process. 2018;27(5):2217-2228.
12. Zeng B. Optimal median-type filtering under structural constraints. IEEE Trans Image Process. 1995;4(7):921-31.
13. Chandrinos A. Aspects of automated perimetry * publisher: LAP LAMBERT Academic Publishing; 2020. ISBN: 978-620-2-56290
14. Betz-Stablein BD, Morgan WH, House PH, Hazelton ML. Spatial modelling of visual field data for assessing glaucoma progression - investigative ophthalmology & visual science. 2013;54:1544-1553.
15. Gardiner SK, Crabb DP, Fitzke FW, Hitchings RA. Reducing noise in suspected glaucomatous visual fields by using a new spatial filter. Vision Research. 2004;839 – 848.
16. Gardiner SK, Swanson WH, Demirel S. The effect of limiting the range of perimetric sensitivities on pointwise assessment of visual field progression in glaucoma. Invest Ophthalmol Vis Sci. 2016;1:57(1):288-94.
17. Nevalainen J, Paetzold J, Papageorgiou E, Sample P, et al. Pamela A. Specification of progression in glaucomatous visual field loss, applying locally condensed stimulus arrangements Graefe's Archive for Clinical and Experimental Ophthalmology. 2009; 247:1659.

18. Kirwan JF , Hustler A, Bobat H, Toms L, Crabb DP, McNaught A. Portsmouth visual field database: An audit of glaucoma progression – Eye. 2014; 28:974–979.
19. Fitzke FW, Crabb DP, McNaught AI, et al. Image processing of computerised visual field data.: Br J Ophthalmol. 1995;79:207–12.
20. Crabb DP, Fitzke FW, McNaught AI, Edgar DF, Hitchings RA. Improving the prediction of visual field progression in glaucoma using spatial processing. Ophthalmology. 1997;104(3):517–524.
21. Crabb DP, Gardiner SK., Fitzke FW, Hitchings RA. A new spatial filter for visual field data p.31 Perimetry Update 2002/2003 Edited by D. Henson and M. Wall, The Kugler Publications, The Hague, Netherlands; 2003.
22. Morales E, de Leon JMS, Abdollahi N, Yu F, Nouri-Mahdavi K, Caprioli J. Enhancement of visual field predictions with pointwise exponential regression (PER) and pointwise linear regression (PLR) Translational Vision Science & Technology. 2016;5:12.
23. Strouthidis N, Scott A, Viswanathan A, Crabb D, Garway-Heath. Monitoring glaucomatous visual field progression: The effect of a novel spatial filter. Invest Ophthalmol Vis Sci. 2007;48:251-257.
24. Spry P, Johnson C. Identification of progressive glaucomatous visual field loss. Survey of Ophthalmology. 200;(47):158-173.
25. Garway-Heath DF, Poinosawmy D, Fitzke FW, Hitchings RA. Mapping the visual field to the optic disc in normal tension glaucoma eyes. Ophthalmology. 2000; 107(10):1809-1815.
26. Chandrinios A, Tzamouranis DD. A review of learning effect in perimetry ophthalmology research An International Journal. 2020;12(2):23-30.
27. Chen Z, Hu K, Carpena P, Bernaola-Galvan P, Stanley HE, Ivanov PCh. Effect of nonlinear filters on detrended fluctuation analysis. Phys Rev E Stat Nonlin Soft Matter Phys. 2005;71(1,1):011104.

APPENDIX

```
% Module One
%<< MatLab module for data retrieve and sensitivity draft>>

function OUT=calcstd(SENS,DATASET);

%calculate std values for sub-groups
% SENS entire set of sensitivity data
% DATASET is input matrix
% OUT includes 6 values for the different regions of the visual field

OUT=ones(6,1);

sup=(1:5,9,10,17);
upper=(6:8,11:16);
temporal=(18,27,36,44);
inf=(37,43,45,46,49:54);
lower=(29:31,38:42,47,48);
nasal=(20:22);

temp=SENS([DATASET],sup(:));
OUT(1)=mean(temp(:));
temp=SENS([DATASET],upper(:));
OUT(2)=mean(temp(:));
temp=SENS([DATASET],temporal(:));
OUT(3)=mean(temp(:));
temp=SENS([DATASET],inf(:));
OUT(4)=mean(temp(:));
temp=SENS([DATASET],lower(:));
OUT(5)=mean(temp(:));
temp=SENS([DATASET],nasal(:));
OUT(6)=mean(temp(:))

% Module Two
%<< This MatLab module draws all visit data (1 to 5) for sensitivity and compare visit 1 with median filter>>

% Display additional eye data

close all
clear all

% Load all the data
load ALL_5_DATA.mat
fname='SENSTODEV1NEWMedian2s';
NH=1; %Neighbourhood

% Data types : PSD, SENS, SENS_add, SHAP, SHHI or TODEV
data=SENS-TODEV;

% auge : left or right eye in auge
% fName : Name of the subject
% fgroup: 1== normal, 2==OAG and 3 == OHT
% id_Bilder :
% strategie :ss, sw or sf
```

```

% visite : one or five

res_sup_mat=ones(4,9);
res_inf_mat=ones(4,9);
res_mat=ones(2370,54);

%%%%%%%%%%%%%%%%%%%%%%%%%%%%%%%%%%%%%%%%%%%%%%%%%%%%%%%%%%%%%%%%%%%%%%%%

h = waitbar(0,'Please wait...');

for lo=1:length(auge),

cur_data=data([lo,:]);

if auge(lo,)=='RA',

%%%%%%%%%%%%%%%%%%%%%%%%%%%%%%%%%%%%%%%%%%%%%%%%%%%%%%%%%%%%%%%%%%%%%%%% Right eye

r_data=ones(8,9);

r_data(1,4:7)=cur_data(1:4);
r_data(2,3:8)=cur_data(5:10);
r_data(3,2:9)=cur_data(11:18);
r_data(4,1:9)=cur_data(19:27);
r_data(5,1:9)=cur_data(28:36);
r_data(6,2:9)=cur_data(37:44);
r_data(7,3:8)=cur_data(45:50);
r_data(8,4:7)=cur_data(51:54);

sup_data=r_data(1:4,:);
pre_sup_data=flipud(sup_data(2:4,:));
post_sup_data=flipud(sup_data(1:3,:));
enl_sup_data=(pre_sup_data;sup_data;post_sup_data);

enl_sup_data(2,1)=enl_sup_data(2,3);
enl_sup_data(3,1:2)=fliplr(enl_sup_data(3,4:5));
enl_sup_data(4,1:3)=fliplr(enl_sup_data(4,5:7));
enl_sup_data(5,1:2)=fliplr(enl_sup_data(5,4:5));
enl_sup_data(6,1)=enl_sup_data(6,3);
enl_sup_data(8,1)=enl_sup_data(8,3);
enl_sup_data(9,1:2)=fliplr(enl_sup_data(9,4:5));
enl_sup_data(10,1:3)=fliplr(enl_sup_data(10,5:7));

enl_sup_data(3,9)=enl_sup_data(3,7);
enl_sup_data(4,8:9)=fliplr(enl_sup_data(4,5:6));
enl_sup_data(5,9)=enl_sup_data(5,7);

enl_sup_data(9,9)=enl_sup_data(9,7);
enl_sup_data(10,8:9)=fliplr(enl_sup_data(10,5:6));

comp_enl_sup_data=(fliplr(enl_sup_data(:,2:4)),enl_sup_data,fliplr(enl_sup_data(:,6:8)));

for i=4:7,
for j=4:12,
res_sup_mat(i-3,j-3)=myfun(comp_enl_sup_data(i-NH:i+NH,j-NH:j+NH));
end
end

```

```

%%%%%%%%%%

inf_data=r_data(5:8,:);
pre_inf_data=flipud(inf_data(2:4,:));
post_inf_data=flipud(inf_data(1:3,:));
enl_inf_data=(pre_inf_data;inf_data;post_inf_data);

enl_inf_data(1,1:3)=fliplr(enl_inf_data(1,5:7));
enl_inf_data(2,1:2)=fliplr(enl_inf_data(2,4:5));
enl_inf_data(3,1)=enl_inf_data(3,3);

enl_inf_data(5,1)=enl_inf_data(5,3);
enl_inf_data(6,1:2)=fliplr(enl_inf_data(6,4:5));
enl_inf_data(7,1:3)=fliplr(enl_inf_data(7,5:7));
enl_inf_data(8,1:2)=fliplr(enl_inf_data(8,4:5));
enl_inf_data(9,1)=enl_inf_data(9,3);

enl_inf_data(1,8:9)=fliplr(enl_inf_data(1,5:6));
enl_inf_data(2,9)=enl_inf_data(2,7);

enl_inf_data(6,9)=enl_inf_data(6,7);
enl_inf_data(7,8:9)=fliplr(enl_inf_data(7,5:6));
enl_inf_data(8,9)=enl_inf_data(8,7);
comp_enl_inf_data=(fliplr(enl_inf_data(:,2:4)),enl_inf_data,fliplr(enl_inf_data(:,6:8)));

for i=4:7,
for j=4:12,
res_inf_mat(i-3,j-3)=myfun(comp_enl_inf_data(i-NH:i+NH,j-NH:j+NH));
end
end
res_mat(lo,1:4)=res_sup_mat(1,4:7);
res_mat(lo,5:10)=res_sup_mat(2,3:8);
res_mat(lo,11:18)=res_sup_mat(3,2:9);
res_mat(lo,19:27)=res_sup_mat(4,1:9);
res_mat(lo,28:36)=res_inf_mat(1,1:9);
res_mat(lo,37:44)=res_inf_mat(2,2:9);
res_mat(lo,45:50)=res_inf_mat(3,3:8);
res_mat(lo,51:54)=res_inf_mat(4,4:7);

res_mat(lo,:)=cr_hybrid(cur_data,res_mat(lo,:));

elseif auge(lo,:)=='LA',
%%%%%%%%%% Left eye
l_data=ones(8,9);

l_data(1,3:6)=fliplr(cur_data(1:4));
l_data(2,2:7)=fliplr(cur_data(5:10));
l_data(3,1:8)=fliplr(cur_data(11:18));
l_data(4,1:9)=fliplr(cur_data(19:27));
l_data(5,1:9)=fliplr(cur_data(28:36));
l_data(6,1:8)=fliplr(cur_data(37:44));
l_data(7,2:7)=fliplr(cur_data(45:50));
l_data(8,3:6)=fliplr(cur_data(51:54));

sup_data=l_data(1:4,:);
pre_sup_data=flipud(sup_data(2:4,:));

```

```

post_sup_data=flipud(sup_data(1:3,:));
enl_sup_data=(pre_sup_data;sup_data;post_sup_data);

enl_sup_data(3,1)=enl_sup_data(3,3);
enl_sup_data(4,1:2)=fliplr(enl_sup_data(4,4:5));
enl_sup_data(5,1)=enl_sup_data(5,3);
enl_sup_data(9,1)=enl_sup_data(9,3);
enl_sup_data(10,1:2)=fliplr(enl_sup_data(10,4:5));

enl_sup_data(2,9)=enl_sup_data(2,7);
enl_sup_data(3,8:9)=fliplr(enl_sup_data(3,5:6));
enl_sup_data(4,7:9)=fliplr(enl_sup_data(4,3:5));
enl_sup_data(5,8:9)=fliplr(enl_sup_data(5,5:6));
enl_sup_data(6,9)=enl_sup_data(6,7);

enl_sup_data(8,9)=enl_sup_data(8,7);
enl_sup_data(9,8:9)=fliplr(enl_sup_data(9,5:6));
enl_sup_data(10,7:9)=fliplr(enl_sup_data(10,3:5));
comp_enl_sup_data=(fliplr(enl_sup_data(:,2:4)),enl_sup_data,fliplr(enl_sup_data(:,6:8)));

for i=4:7,
for j=4:12,
res_sup_mat(i-3,j-3)=myfun(comp_enl_sup_data(i-NH:i+NH,j-NH:j+NH));
end
end

inf_data=l_data(5:8,:);
pre_inf_data=flipud(inf_data(2:4,:));
post_inf_data=flipud(inf_data(1:3,:));
enl_inf_data=(pre_inf_data;inf_data;post_inf_data);

enl_inf_data(1,1:2)=fliplr(enl_inf_data(1,4:5));
enl_inf_data(2,1)=enl_inf_data(2,3);
enl_inf_data(6,1)=enl_inf_data(6,3);
enl_inf_data(7,1:2)=fliplr(enl_inf_data(7,4:5));
enl_inf_data(8,1)=enl_inf_data(8,3);

enl_inf_data(1,7:9)=fliplr(enl_inf_data(1,3:5));
enl_inf_data(2,8:9)=fliplr(enl_inf_data(2,5:6));
enl_inf_data(3,9)=enl_inf_data(3,7);

enl_inf_data(5,9)=enl_inf_data(3,7);
enl_inf_data(6,8:9)=fliplr(enl_inf_data(6,5:6));
enl_inf_data(7,7:9)=fliplr(enl_inf_data(7,3:5));
enl_inf_data(8,8:9)=fliplr(enl_inf_data(8,5:6));
enl_inf_data(9,9)=enl_inf_data(9,7);
comp_enl_inf_data=(fliplr(enl_inf_data(:,2:4)),enl_inf_data,fliplr(enl_inf_data(:,6:8)));

for i=4:7,
for j=4:12,
res_inf_mat(i-3,j-3)=myfun(comp_enl_inf_data(i-NH:i+NH,j-NH:j+NH));
end
end

res_mat(lo,1:4)=res_sup_mat(1,3:6);
res_mat(lo,5:10)=res_sup_mat(2,2:7);

```



```
%  
temp=find(res_mat(upper)<cur_data(upper));  
hybrid(upper(temp))=cur_data(upper(temp))-2.37;  
temp=find(res_mat(upper)>cur_data(upper));  
hybrid(upper(temp))=cur_data(upper(temp))+2.37;  
temp=find(res_mat(upper)==cur_data(upper));  
hybrid(upper(temp))=cur_data(upper(temp));  
%  
temp=find(res_mat(temporal)<cur_data(temporal));  
hybrid(temporal(temp))=cur_data(temporal(temp))-1.6;  
temp=find(res_mat(temporal)>cur_data(temporal));  
hybrid(temporal(temp))=cur_data(temporal(temp))+1.6;  
temp=find(res_mat(temporal)==cur_data(temporal));  
hybrid(temporal(temp))=cur_data(temporal(temp));  
%  
temp=find(res_mat(Inf)<cur_data(Inf));  
hybrid(Inf(temp))=cur_data(Inf(temp))-2.27;  
temp=find(res_mat(Inf)>cur_data(Inf));  
hybrid(Inf(temp))=cur_data(Inf(temp))+2.27;  
temp=find(res_mat(Inf)==cur_data(Inf));  
hybrid(Inf(temp))=cur_data(Inf(temp));  
%  
temp=find(res_mat(lower)<cur_data(lower));  
hybrid(lower(temp))=cur_data(lower(temp))-2.37;  
temp=find(res_mat(lower)>cur_data(lower));  
hybrid(lower(temp))=cur_data(lower(temp))+2.37;  
temp=find(res_mat(lower)==cur_data(lower));  
hybrid(lower(temp))=cur_data(lower(temp));  
%  
temp=find(res_mat(nasal)<cur_data(nasal));  
hybrid(nasal(temp))=cur_data(nasal(temp))-2.76;  
temp=find(res_mat(nasal)>cur_data(nasal));  
hybrid(nasal(temp))=cur_data(nasal(temp))+2.76;  
temp=find(res_mat(nasal)==cur_data(nasal));  
hybrid(nasal(temp))=cur_data(nasal(temp));  
  
hybrid(keep_values)=cur_data(keep_values);  
  
%%%%%%%%%
```

© 2021 Chandrinos; This is an Open Access article distributed under the terms of the Creative Commons Attribution License (<http://creativecommons.org/licenses/by/4.0>), which permits unrestricted use, distribution, and reproduction in any medium, provided the original work is properly cited.

Peer-review history:
The peer review history for this paper can be accessed here:
<http://www.sdiarticle4.com/review-history/63816>